

A measurement of two-photon exchange in unpolarized elastic electron–proton scattering

J. Arrington (Spokesperson), D. F. Geesaman, K. Hafidi, R. J. Holt
H. E. Jackson, D. H. Potterveld, P. E. Reimer, E. C. Schulte, X. Zheng
Argonne National Laboratory, Argonne, IL

M. E. Christy, C. E. Keppel
Hampton University, Hampton, VA

G. Niculescu, I. Niculescu
James Madison University, Harrisonburg, VA

P. E. Bosted, R. Ent, D. Gaskell, A. F. Lung, D. J. Mack, D. G. Meekins, G. Smith
Jefferson Laboratory, Newport News, VA

R. E. Segel, I. Qattan
Northwestern University, Evanston, IL

R. Asaturyan, H. Mkrtchyan, V. Tadevosyan, T. Navasardyan
Yerevan Physics Institute, Armenia

(Dated: December 6, 2004)

Abstract

We propose a series of high precision measurements of elastic electron–proton scattering over a wide kinematic range to extract the ε and Q^2 dependence of the two-photon exchange contributions. These data will allow a precise determination of the difference between Rosenbluth and polarization transfer measurements and hence the Q^2 dependence of the two-photon exchange effects for $0.9 < Q^2 < 6.6$ GeV². At low Q^2 values, we are directly sensitive only to the *nonlinear* portion of the two-photon exchange contributions. Based on recent calculations of the two-photon exchange terms, we expect that the measurement will be able to observe nonlinearities of more than four standard deviations at both $Q^2 = 1.12$ and 2.56 GeV². At large Q^2 , G_E becomes small enough that the reduced cross section in the Born approximation has almost no ε dependence. In this region, measurements of the ε dependence are sensitive to the *full* two-photon exchange contributions. Such measurements are nearly as clean as comparisons of electron–proton and positron–proton scattering which at present cannot be extended to large Q^2 values.

While most discussions of two-photon exchange have centered around their impact on Rosenbluth determinations of G_E , they also have significant effects on polarization transfer measurements of G_E and Rosenbluth extractions of G_M . Without additional constraint on two-photon exchange, there remain large uncertainties in our knowledge of both G_E and G_M . The proposed measurements, combined with existing data, will allow us to extract these two-photon exchange amplitudes which can then be used to correct the measured form factors. In addition, it is important to further develop models of two-photon exchange effects in elastic e – p scattering, where we have the opportunity to make direct measurements of these effects. Improving our understanding of these effects is crucial in determining how they might impact other high precision measurements.

I. INTRODUCTION

The striking difference between Rosenbluth [1, 2] and polarization transfer [3, 4] measurements of the proton electromagnetic form factors has led to significant activity aimed at understanding and resolving this discrepancy. A reanalysis of existing form factor measurements [5], combined with new, high-precision Rosenbluth measurements from JLab E01-001 [6], rule out the kind of experimental error suggested when the discrepancy was first observed. At present, the explanation appears to be the effects of two-photon exchange (TPE) [7–9]. **If two-photon exchange corrections do explain the discrepancy then our knowledge of the form factors is limited by our poor understanding of the (potentially large) TPE effects on polarization transfer measurements of G_E and Rosenbluth measurements of G_M .**

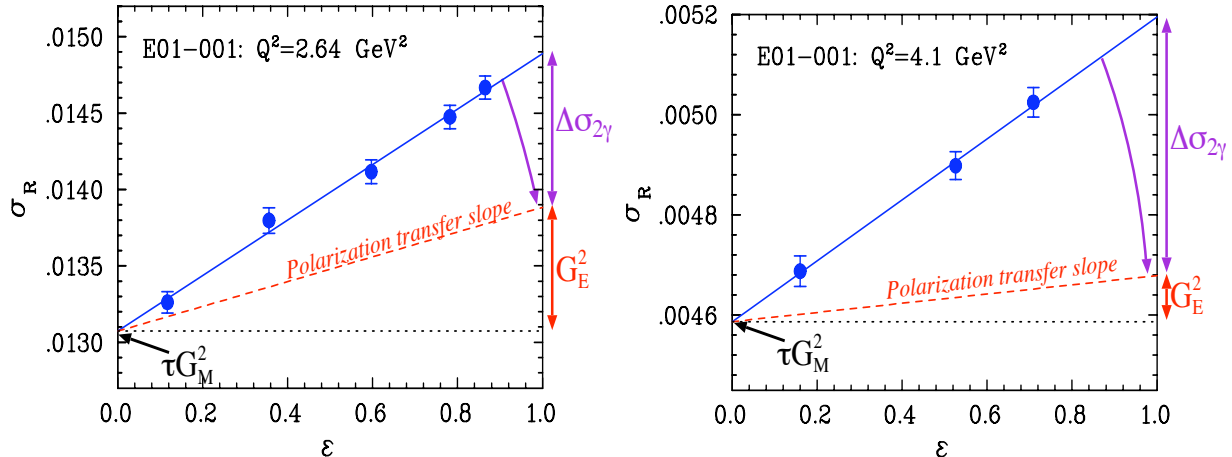


FIG. 1: The ε dependence of the reduced cross section as predicted from the polarization transfer results for G_E/G_M (red dashed line), and as measured in JLab E01-001 (circles). If the polarization transfer represents the true form factors, TPE yields more than half of the ε dependence at 2.64 GeV^2 , and 85% at 4.1 GeV^2 .

Analyses of the discrepancy that assume it is due primarily to missing corrections in the cross section measurements [5, 7, 10] indicate that the difference could be explained by an error in the ε dependence of the cross section of approximately 5–8% for $1 < Q^2 < 6 \text{ GeV}^2$. The correction would have to be close enough to linear that it does not spoil the linearity expected from the Rosenbluth formula, as shown in Figure 1. Coulomb distortion does modify the ε dependence of the cross section, but has a small effect relative to the observed discrepancy [11, 12]. For the most part, investigations have focussed on the effect of TPE corrections [7, 8, 13–15] beyond those included in the traditional calculations of radiative corrections. If the discrepancy is due to TPE and the polarization transfer results are

approximately correct, then $\mu_p G_E/G_M$ becomes small enough that the ε dependence is dominated by TPE effects for $Q^2 > 3\text{--}4 \text{ GeV}^2$ (Fig. 1). **For these measurements, we will make a nearly background-free extraction of TPE effects at Q^2 values well above the region where we can make precise comparisons of positron and electron scattering.**

The impact of two-photon exchange goes beyond its impact on our understanding of the proton electromagnetic structure. At large Q^2 , the discrepancy implies cross section differences of 5–10%. While the effect of TPE on G_E is small at low Q^2 values, their effect on the *cross section* may still be significant at low Q^2 (below 1 GeV^2). Precise knowledge of these form factors is needed as input for many experiments, to determine experimental normalization [16], parameterize the elastic $e\text{--}p$ cross section in $A(e, e'p)$ measurements [17], or extract additional form factors in parity violating electron or $\nu\text{--}A$ scattering [10, 18, 19]. **For these high-precision measurements, it is critical to have reliable knowledge of both the proton form factors and two-photon exchange contributions.**

Finally, the observation of large TPE effects in elastic $e\text{--}p$ scattering raises the broader issue of TPE effects in other electron scattering measurements. While TPE diagrams have been calculated exactly for scattering from a structureless target (e.g. DIS scattering from a quark), the calculations are much more difficult for elastic $e\text{--}n$, $e\text{--}A$, and transition form factors measurements. Elastic $e\text{--}p$ scattering provides a critical testing ground for models of TPE, as it is the only case where it is currently possible to make precision measurements of TPE effects. **As yet, there is no calculation of TPE that explains the observed discrepancy in $e\text{--}p$ scattering, and the calculations that do exist predict significantly different ε dependences. Without additional data to constrain and improve these models, we cannot rely on them to identify potential TPE effects in other reactions.**

II. SIGNATURES OF TWO-PHOTON EXCHANGE CONTRIBUTIONS

Two-photon exchange contributions to elastic electron–proton scattering can be observed in several different ways. The real part of the TPE amplitude modifies both the unpolarized cross section and the polarization transfer components used to extract G_E/G_M . The imaginary part of the amplitude leads to non-zero values for the Born-forbidden observables A_y and P_N . These observables provide clean measurements of two-photon effects, but are not directly connected to the discrepancy in the form factors.

A. Positron to electron comparisons

In principle, the cleanest way to examine the effects of two-photon corrections in the unpolarized e - p cross section is to compare positron-proton and electron-proton scattering. Interference terms between one-photon and two-photon exchange have opposite signs for positron and electron scattering, and so yield a measurable difference. Early comparisons between e^+p and e^-p scattering [20], as well as μ^+p and μ^-p [21], were interpreted as showing that the two-photon corrections were extremely small ($<1\%$). However, the low intensity of the positron (and muon) beams has made precise measurements nearly impossible for large Q^2 or small ε . There is some evidence of a charge-dependent term to the $e^\pm p$ elastic cross section at small values of ε [22], but the data at low ε is not very precise and is limited to Q^2 values well below the region of the observed discrepancy.

One would like to make high precision electron-positron comparisons at small ε values over a large range in Q^2 . There are plans to make additional comparisons at low ε values [23, 24], but they will cover a limited Q^2 range and will be not able to provide precise data at the Q^2 values where there is a clear discrepancy in the extraction of the form factors. However, they will be important in verifying that the discrepancy is caused by TPE and can provide clean information on TPE measurements at low-to-moderate Q^2 values.

B. Experimental limits on nonlinearities

In the Born approximation, the reduced cross section depends linearly on ε . Any deviation from linearity must come from higher order terms that are not included in the standard radiative correction procedures. At lower Q^2 values, observing such a deviation would provide a clear signature of two-photon exchange, and would provide information on the *nonlinear* component of the TPE. At large Q^2 values, above 3-4 GeV², G_E becomes small enough that almost all of the ε dependence comes from TPE, as shown in Fig. 1. In this region, the ε dependence of the reduced cross section provides a clean measurement of the TPE contributions.

To compare the proposed measurements to previous linearity tests, we need to define a figure of merit for these measurements. For a fit of the form

$$\sigma_R = P_0[1 + P_1\varepsilon + P_2\varepsilon^2], \quad (1)$$

P_2 provides a simple measure of the relative size of nonlinear terms, and δP_2 can be used to set limits on ε^2 terms. Conventional Rosenbluth separation measurements have found P_2 to be consistent with zero, and the best measurement [25] yields $\delta P_2 \approx 10\%$. The recent

results from E01-001 [6], obtained by detecting the struck proton rather than the scattered electron, yield much better limits on P_2 .

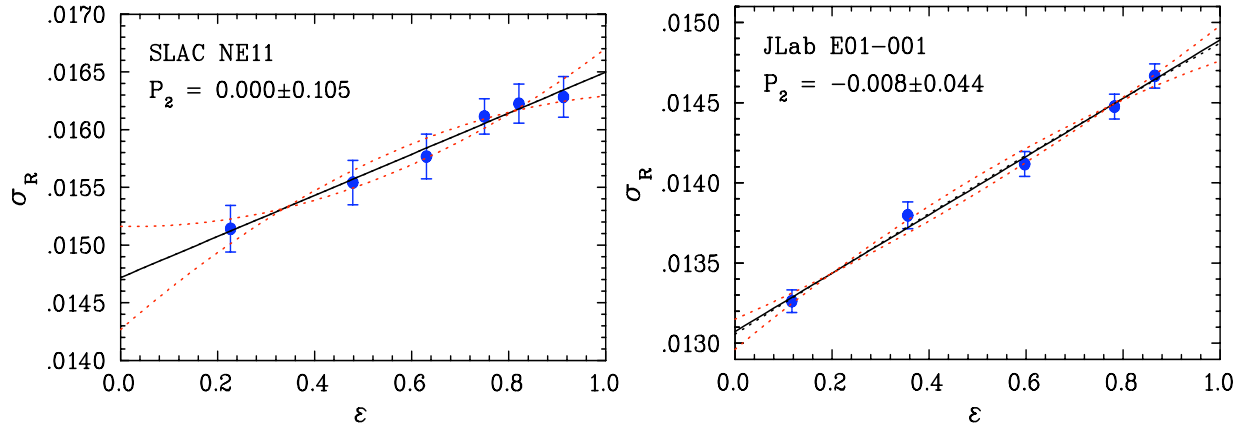


FIG. 2: The ε dependence of the reduced cross section from NE11 (using only data from the 8 GeV spectrometer). The solid line is the linear fit, while the dashed lines are quadratic fits with $P_2 = \pm 0.105$ for NE11, $P_2 = -0.008 \pm 0.044$ for E01-001 (1σ variations on the central value).

Figure 2 shows the reduced cross section as a function of ε for the best conventional Rosenbluth separation (SLAC NE11 [25]), and from E01-001 [6]. Figure 3 shows the values of P_2 extracted from all previous measurements (including the new E01-001 results), compared to the limits that can be set by this proposal. The proposed measurements will improve the limits on P_2 by more than a factor of five for $Q^2 < 2 \text{ GeV}^2$, and by a factor of two to three for larger Q^2 values.

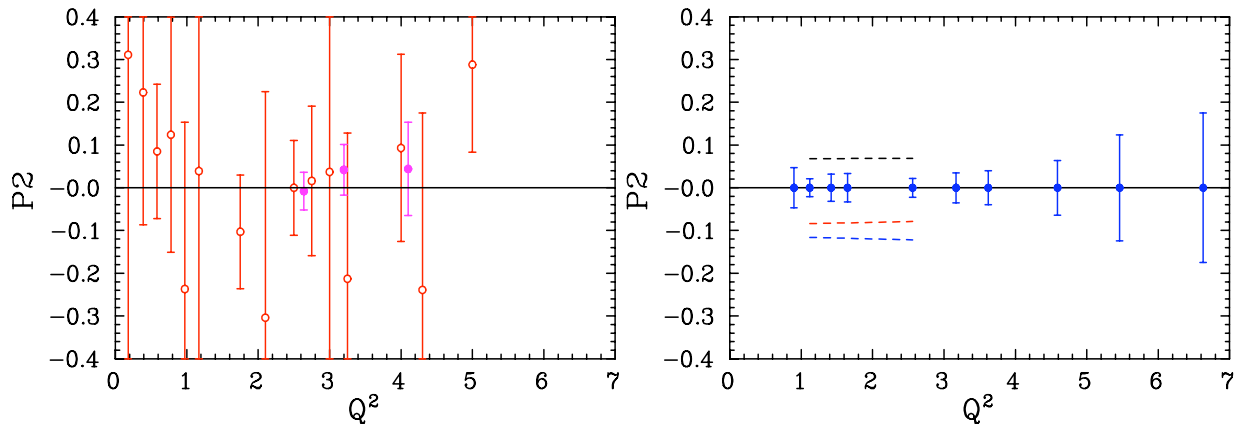


FIG. 3: Left: The value and uncertainty for P_2 from published Rosenbluth separations (hollow circles) and the new E01-001 results (solid circles). The limit on P_2 is $2.9 \pm 5.5\%$ (combining all published results) or $1.3 \pm 3.4\%$ (including E01-001). Right: projected uncertainties for this proposal, with a combined uncertainty of $\delta P_2 = 1.1\%$. The dashed lines represent the predictions based three of the models discussed in Sec. III (the colors match those in Fig. 6)

While the limit on the curvature parameter P_2 provides a reasonable figure of merit,

it does not fully represent the sensitivity of the tests. The previous measurements have almost no precise data for $\varepsilon < 0.2$, and thus have very little sensitivity to nonlinearities that occur only at low ε . For a precise measurement of nonlinearities, it is important to covering the maximum possible ε range so that one is sensitive to nonlinearities at both large and small ε values, and to have enough ε in the linear region to act as a precise baseline for deviations from linearity. It should be noted that most calculations of TPE indicate that the nonlinear terms are likely appear as $\varepsilon \rightarrow 0$ or $\varepsilon \rightarrow 1$. Thus, maximizing the ε range of the measurements is extremely important.

III. ESTIMATES OF TWO-PHOTON EXCHANGE CORRECTIONS

In the 1950s and 1960s, several papers estimated the size of two-photon contributions to the unpolarized cross sections, using only the proton intermediate state [26], and including excited intermediate states [27–30]. These calculations predicted TPE effects consistent with the small differences between positron and electron scattering. More recently, a significant amount of work has gone into improving such calculations [8, 14, 15]. All of the new calculations predict observable nonlinearities in the ε dependence of the TPE corrections.

A. Recent calculations of two-photon exchange

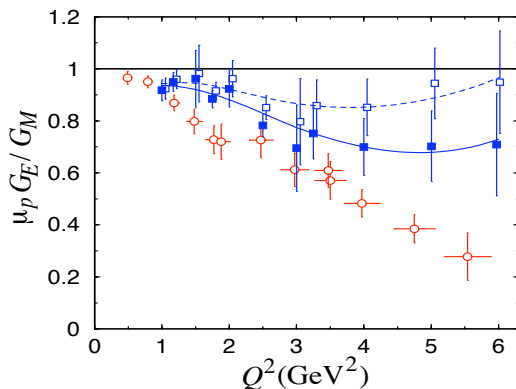


FIG. 4: The effect of Blunden, et al., on Rosenbluth extractions of $\mu_p G_E / G_M$ (from Ref. [8]). Hollow squares indicate $\mu_p G_E / G_M$ as measured, solid squares after applying the TPE correction.

Calculations by Blunden, Melnitchouk, and Tjon [8] yield an ε dependence of approximately 2%, with small nonlinearities at low ε values and a weak Q^2 dependence. This calculation includes only the elastic portion of the two-photon correction; the box and crossed-box diagrams with the proton in the intermediate state, and neglect excited intermediate states.

With the inclusion of improved form factors, these corrections increase to 3% [31]. Figure 4 shows the effect of this calculation on Rosenbluth extractions of G_E/G_M . While the discrepancy is largely resolved for $Q^2 = 2\text{--}3 \text{ GeV}^2$, this calculation does not describe the discrepancy at lower or higher Q^2 values.

A more recent work by Chen, et al. [15], calculates the two-photon exchange effect at the quark-parton level, using a generalized parton distribution to describe the emission and re-absorption of the partons by the nucleon. While this approach is not expected to be valid at low Q^2 or ε values, the calculations for higher Q^2 again show a significant ε dependence (and nonlinearity) to the correction, with only a weak Q^2 dependence. While it has been asserted that this calculation fully explains the discrepancy, the correction is in fact only half of what is necessary to resolve the discrepancy (Fig. 5).

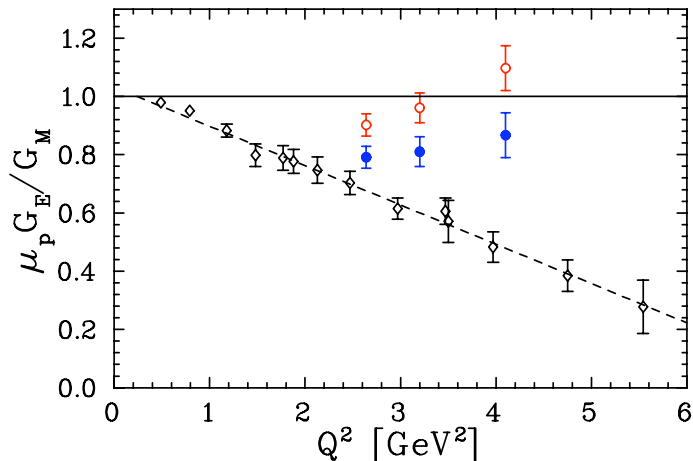


FIG. 5: Left: The values of $\mu_p G_E/G_M$ as measured by E01-001, before (hollow) and after (solid) applying the corrections from Chen, et al. [15]

Calculations at the quark-parton level in the double logarithm approximation by Afanasev, et al. [14] yield a different form for the ε dependence, with nonlinearities appearing at large ε . However, it yields a very different nonlinearity from the calculation of Ref. [8]. In addition, it predicts only the ε and Q^2 dependence, but not the overall magnitude.

Finally, Rekaló and Tomasi-Gustafsson [13] predict that the TPE corrections should depend on $x = \sqrt{1+\varepsilon}/\sqrt{1-\varepsilon}$ based on symmetry arguments. They predict a similar ε dependence to Afanasev, et al., but do not calculate the size or Q^2 dependence.

Because the first two calculations yield roughly half of the effect needed to explain the discrepancy, and because the others have arbitrary scale factors, we normalize the calculations so that the correction is large enough to explain the discrepancy. We then use these scaled calculations to estimate the likely size of the nonlinearities we might observe. Fig-

ure 6 shows the ε dependence for these calculations for $Q^2=2-3$ GeV². For Ref. [15], the calculation is not expected to be valid at low Q^2 or ε values, and so we show the calculation for $Q^2 = 5$ GeV², and have extended the curve linearly below $\varepsilon = 0.26$.

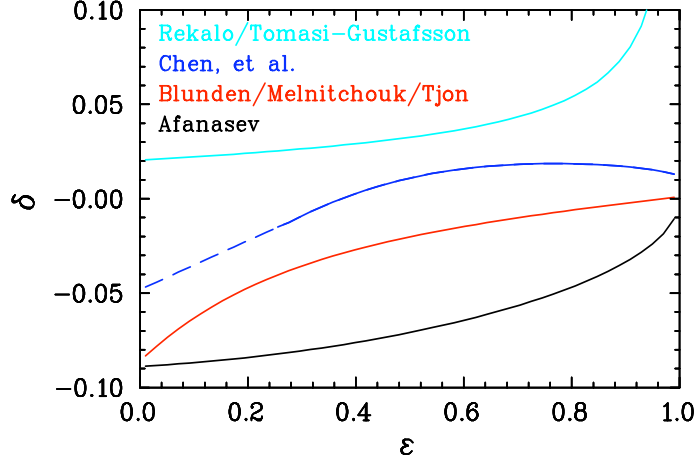


FIG. 6: The two-photon exchange contribution, $\delta = (\sigma_{2\gamma} - \sigma_{1\gamma})/\sigma_{1\gamma}$, to the elastic $e-p$ cross section from the calculations of Rekalo, et al., [13], Chen, et al., [15], Blunden, et al., [31], and Afanasev, et al. [14], after scaling the calculations to yield a ε dependence of approximately 6% over the ε range of existing data.

These calculations make very different predictions for both the size and ε range of the nonlinearities. The calculations of Afanasev, et al. and Rekalo, et al., show large nonlinearities as $\varepsilon \rightarrow 1$ values, while the calculation of Blunden, et al., shows similar nonlinearities for $\varepsilon \rightarrow 0$. The calculation of Chen, et al., has slightly smaller deviations from linearity, but they occur at both intermediate and large ε values. Note that even the sign of the curvature parameter P_2 differs in the different approaches. Even if we exclude the form of Rekalo, et al., which appears to be ruled out by existing data, the range of predictions is ten times larger than the sensitivity of the projected measurements at $Q^2=2.56$ GeV², and nearly twenty times larger than the combined limit for the proposed measurements.

B. Estimated impact on the proton form factors

If TPE explains the discrepancy, it must be largely due to a modification of the ε dependence of the reduced cross section, leading to a significant overestimate of G_E in Rosenbluth extractions, as illustrated in Fig. 1. However, the two-photon exchange amplitudes can also have significant effects on the polarization transfer data and the Rosenbluth extraction of G_M , and thus our knowledge of the form factors is limited by how well we can extract these TPE corrections.

Most of the calculations described above predict that the largest effect on the cross section occurs for small ε values, and would thus predict that measurements of G_M at $\varepsilon = 0$ would be reduced by roughly 3-5% at large Q^2 , with little Q^2 dependence. However, while these calculations have been normalized to yield approximately the same *average* ε dependence, they yield very different corrections to the form factors extracted from data in different ε ranges. For example, the calculation of Chen, et al., has little ε dependence for $\varepsilon > 0.5$, and so would yield very little modification to Rosenbluth extractions of G_E that are dominated by data at large ε values [1, 32–34].

The TPE corrections also lead to a modification in G_M , which again depends strongly on the ε range of the data. While the calculation of Chen, et al., does have a significant effect on G_M if measured directly by taking data for very low ε values, the effect will be minimal (or even of the opposite sign) for data limited to large ε values. In contrast to this, the calculations of Afanasev, et al. and Rekalov, et al., will yield *larger* corrections to G_M in data that is limited to large ε values. It is therefore important to know the exact ε dependence of the correction, rather than just the *average* slope.

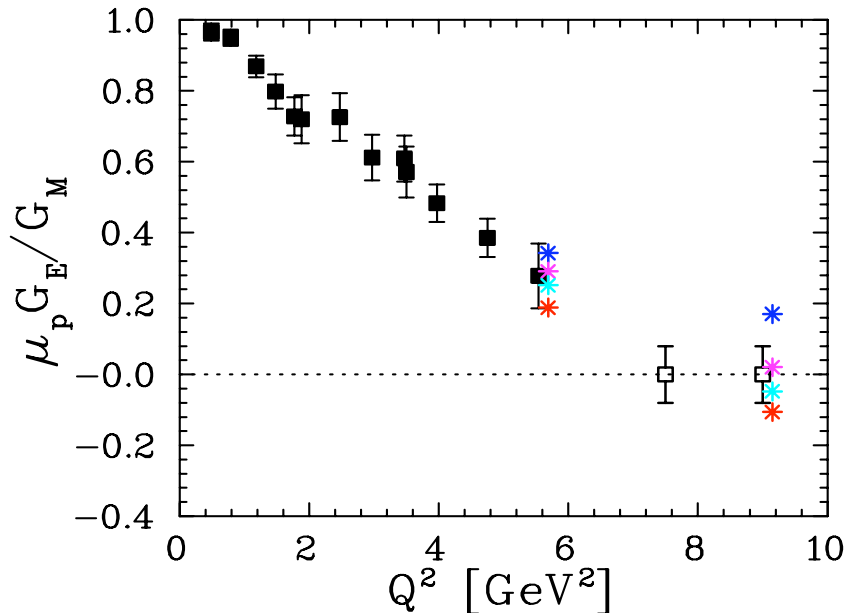


FIG. 7: Polarization transfer extractions of $\mu_p G_E / G_M$ from published measurements (solid squares) and the projected uncertainties for E04-108 (hollow squares). For two points, we have shown the result after applying corrections from various models of TPE (offset in Q^2 for clarity). The top and bottom points show the corrected ratio based on phenomenological analyses of the discrepancy taken from the E04-019 proposal (top-blue) and from Ref. [9] (bottom-red), both of which are discussed in section VB. The middle points are based on the calculations of Refs. [15] (magenta) and [8] (cyan). Note that these are the *unscaled* versions of these calculations, both of which significantly underpredict the effect on the Rosenbluth form factors.

Finally, TPE can also modify the result of the polarization transfer extraction of G_E . The potential size of these TPE effects is illustrated in Figure 7, which shows the existing and projected polarization transfer measurements for $\mu_p G_E/G_M$, along with corrections to $\mu_p G_E/G_M$ for two Q^2 points based on four different models of the TPE effects: two of the calculations discussed in the previous section, and two phenomenological extractions of TPE effects based on the observed discrepancy (described in Sec. VB). If one estimates the uncertainties in the TPE corrections based on just the *scatter* of these different models (ignoring the relatively large experimental uncertainties in the *extractions* of these amplitudes for the two extreme models), the uncertainty is as large or larger than the uncertainty in the polarization transfer measurements. For the largest Q^2 where polarization transfer data is presently available, there is a difference of nearly a factor of two between the largest and smallest results for the corrected value of G_E/G_M . At the highest Q^2 value of the E04-108 (GEp-III), there is a difference of 0.3 between the largest and smallest values of $\mu_p G_E/G_M$. It is of great interest to determine if G_E crosses zero, as predicted by some models, or if it stays positive, as required if we are in the perturbative region. The TPE corrections could be large enough to make the extracted value of G_E/G_M negative (positive), even if the real value of G_E is positive (negative). Thus, it may be impossible to determine if G_E becomes negative without a better understanding of TPE.

IV. EXPERIMENT

We propose to make a series of high-precision Rosenbluth separation measurements to map out the ε and Q^2 dependence of the TPE contributions to the elastic $e-p$ cross section. We will obtain very high precision in these measurements by detecting the struck proton, rather than the scattered electron. Experiment E01-001 [6] has already demonstrated that proton detection allows a much greater precision in extracting the ε dependence of the cross section, and thus form factor ratio G_E/G_M .

The first goal of the proposed experiment is to make improved measurements of any nonlinearities in the ε dependence. The best limit on curvature from conventional Rosenbluth measurements yields $|P_2| < 10\%$. E01-001 reduced this to 4.4% at $Q^2 = 2.64 \text{ GeV}^2$. The proposed measurements would be able to measure P_2 with an uncertainty $\delta P_2 = 0.020$ (0.018) for $Q^2 = 2.56 \text{ GeV}^2$ (1.12 GeV^2). It would also significantly increase the sensitivity at very large and small values of ε . The proposed measurements have a sensitivity of four standard deviations to each of the forms shown in Fig 6. In addition, while the curvature of the quadratic fit is a useful general measure of the nonlinearities, we will provide better

discrimination against specific models.

The second goal is to provide additional, high precision, Rosenbluth separations for $1 \lesssim Q^2 \lesssim 6 \text{ GeV}^2$. This will allow a more precise extraction of the two-photon effects from the difference between Rosenbluth and polarization transfer measurements. The proposed measurement will provide the ε dependence of the correction to the cross section data, either by measuring nonlinearities, or by setting tight limits on deviations from linearity. In addition, it will allow a determination of the Q^2 dependence of the two-photon effects by providing improved Rosenbluth measurements of $\mu_p G_E/G_M$. The proposed measurements will increase the precision on G_E/G_M by a factor of two to three over the entire Q^2 range compared to a global Rosenbluth extraction of the world's body of high- Q^2 cross section data. This will allow a precise comparison with polarization transfer measurements and, combined with limits from existing positron-proton data, will allow us to extract TPE effects well enough to correct the extracted values of G_E and G_M for two-photon contributions (see Sec. VB).

A. Experimental overview

The experiment is proposed for Hall C using the HMS spectrometer and the standard cryogenic targets. Main data taking will be performed at $100 \mu\text{A}$ at beam energies between 0.9 and 6.0 GeV. The 4 cm liquid hydrogen target will be viewed at a maximum angle of 60 degrees, so target length effects on the acceptance (after our solid angle and momentum acceptance cuts) will be negligible. Time of flight and an Aerogel detector will be used for p/π separation. Solid angles will be restricted to 3.2 msr by software cuts to maintain 100% acceptance. Coincidence data will be taken at three settings to check our modeling of the background, the spectrometer resolution, and the radiative tail for the elastic peak.

B. Advantages of proton detection

Table I compares the electron kinematics to the proton kinematics for the two Q^2 values where we propose to make precise linearity tests while Fig. 8 shows the ε dependence of the cross section and sensitivity to scattering angle as a function of ε . Corrections which depend on proton momentum will have no ε dependence, while those which depend on rate will have a much smaller dependence. There is also a significantly smaller ε dependence to the bremsstrahlung correction, and thus a smaller correction that must be applied to the extraction of G_E/G_M . As demonstrated by E01-001 [6], this allows for a much higher

precision in extracting G_E/G_M and examining the ε dependence of the cross section. There are some corrections that are larger when detecting the proton. However, these yield uncertainty mainly in the *absolute* cross section, and have negligible effect on the extraction of the ε dependence.

	$Q^2 = 1.12 \text{ GeV}^2$ settings		$Q^2 = 2.56 \text{ GeV}^2$ settings	
	Proton	Electron	Proton	Electron
ε	0.05–0.98	0.05–0.98	0.08–0.93	0.08–0.93
p [GeV/c]	1.21	0.34–5.47	2.10	0.46–4.70
σ_{min}	3.9 nb/sr	0.30 nb/sr	0.30 nb/sr	0.014 nb/sr
$\sigma_{max}/\sigma_{min}$	2.5	370	1.7	140
$\Delta\sigma/\Delta\theta$	0.4–1.6 %/mr	-(0.1–4.2)%/mr	0.7–1.7 %/mr	-(0.1–2.8)%/mr

TABLE I: Comparison of electron and proton kinematics for the $Q^2=1.12 \text{ GeV}^2$ and $Q^2 = 2.56 \text{ GeV}^2$ measurements.

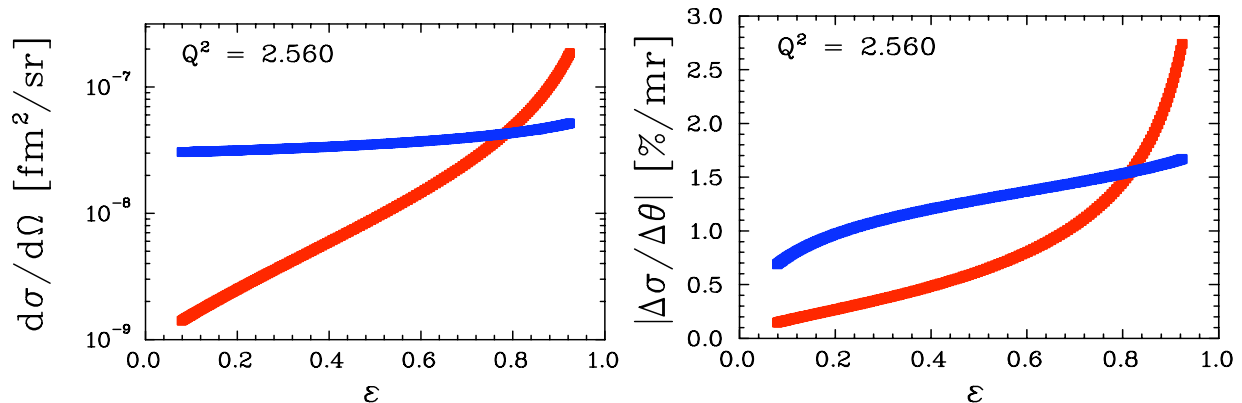


FIG. 8: Cross section (left) and sensitivity to angle (right) for detection of electrons (red) and protons (blue) at $Q^2 = 2.56 \text{ GeV}^2$.

C. Backgrounds

Figure 9 shows simulated proton singles spectra as a function of δp , the difference between the measured proton momentum and the proton momentum calculated from the measured angle (assuming elastic kinematics). The size of the background contributions is matched to the results obtained from E01-001. The elastic events peak near zero, and have a small radiative tail (blue points). These events sit on top of a background of events coming from the target endcaps (yellow). In addition, there are protons coming from Compton scattering (magenta) and neutral pion photoproduction (green).

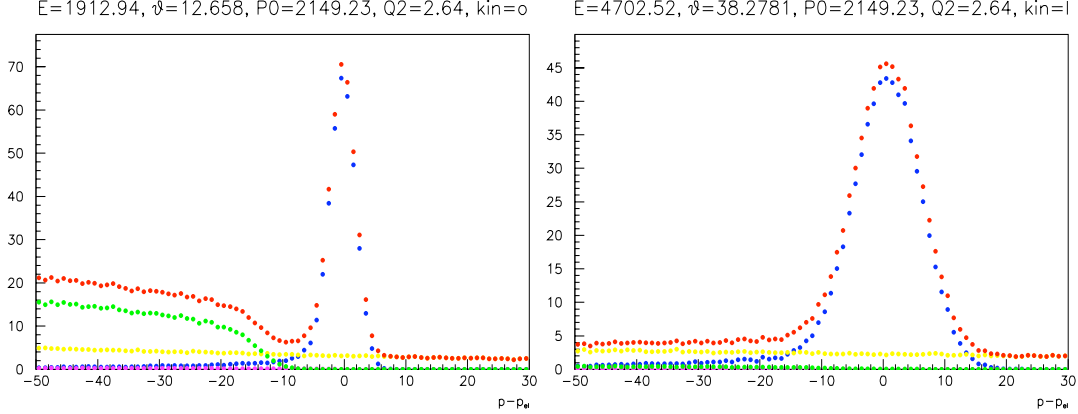


FIG. 9: HMS proton elastic singles spectra from SIMC. The kinematics are taken from the lowest (left) and highest (right) ε points from E01-001 at $Q^2=2.64$ GeV². The points show the dummy target yields (yellow), the simulated Compton (magenta), π^0 -p (green), and elastic (blue) protons. The red points show the sum of all processes

The contributions from the target endcaps are somewhat larger than in the case of electron detection, so we will take a larger fraction of the data on an aluminum ‘dummy’ target, and use a target that more closely matches the radiation length of the hydrogen target. For the spectrum at 2.64 GeV², the endcap subtraction varies between $\sim 15\%$ at low ε ($-15 < \delta p < 15$ MeV) and $\sim 10\%$ at high ε ($-25 < \delta p < 25$ MeV). With these δp cuts, we eliminate most of the non-endcap background contributions while staying away from the edges of the elastic peak. The $\sim 5\%$ ε dependence in the background subtraction will be directly measured and subtracted away. We will measure the endcap contribution to better than 2%, yielding an uncertainty in the slope of 0.1%. Contributions to the nonlinearity are even smaller because the size of the dummy subtraction varies approximately linearly with ε .

Photoproduction of neutral pions is the other significant source of high energy protons. Figure 9 shows the simulated spectrum for $Q^2 = 2.64$ GeV². For forward angle settings (small ε), this background is large but can be almost entirely eliminated with a reasonable cut on the elastic peak. At larger angles, the resolution is worse and the background cannot be cut away, but the background is small and can be reliably modeled and subtracted away. To verify our modeling of the background and the shape of the elastic peak, we will have coincidence runs at multiple kinematics which will allow us to separate the elastic events from the background processes and test our calculations of the line shapes.

There is also a background of charged pions (up to a few percent for E01-001). Time of flight will efficiently remove pions for the low Q^2 data, and an Aerogel detector will be used to reject pions where the time of flight is not fully efficient. The pion contamination

Source	Size	$\delta\sigma/\sigma$ total	$\delta\sigma/\sigma$ G_E/G_M	$\delta\sigma/\sigma$ linearity
Statistics [†]	0.1–0.2%	0.1–0.2%	0.1–0.2%	0.1–0.2%
Energy (fixed offset)	0.04%	0.2%	*0.1%	$\ll 0.1\%$
Energy (random)	0.04%	0.2%	0.2%	0.2%
θ_p (fixed offset)	0.30 mr	0.2–0.5%	*0.3%	$< 0.1\%$
θ_p (random)	0.20 mr	0.1–0.3%	0.1–0.3%	0.1–0.3%
Dead Time		0.1%	$< 0.1\%$	$\ll 0.1\%$
Dummy Subtraction		0.2–0.5%	*0.2%	$\ll 0.1\%$
Background Subtraction		0.1–1.0%	*0.3%	$< 0.1\%$
Radiative Corrections		1.2%	0.2%	$\sim 0.1\%$
			*0.2%	
Luminosity		0.6%	0.2%	0.2%
Proton absorption		1.0%	$\ll 0.1\%$	$\ll 0.1\%$
Acceptance		$\sim 2\%$	$\ll 0.1\%$	$\ll 0.1\%$
Efficiency		0.5%	$\ll 0.1\%$	$\ll 0.1\%$
Total		$\sim 2.8\%$	0.42–0.50%	0.38–0.47%
			*0.52%	

* Uncertainty given is on the slope rather than the individual cross sections

[†] 0.3-0.5% uncertainties for the three largest Q^2 values.

TABLE II: Projected uncertainties for the proposed measurement. The error on the extracted G_E/G_M depends on the value of G_E/G_M and is shown in Fig. 11.

will be negligible after the particle identification cuts, while the inefficiency of the cuts for protons depends only on the proton momentum and thus does not introduce any significant uncertainty in the ε dependence.

D. Systematic uncertainties

Because of the high precision required for this measurement, we must ensure that we account for small corrections that are often neglected. In addition, we must separate out uncertainties which lead to a scale offset for all values at a given Q^2 from those which vary randomly from point-to-point, or those which vary linearly with ε . Table II summarizes the uncertainties for the extraction of the cross section, form factor ratio, and the linearity measurements. These uncertainties are slightly better than those achieved in E01-001 [6], due mainly to improved statistics and improved measurements of the backgrounds from endcap scattering. In addition, both the linearity check and the extraction of G_E/G_M will benefit from the improved ε range of this proposal.

Computer dead time corrections are measured in the standard data acquisition system in Hall C with a very small associated uncertainty. Because of the relatively low rates in the experiment (below 30 kHz), the electronic dead time correction is at most 0.2%, and the ε dependence is a factor of two lower. A larger problem is the effect of multiple tracks in the chambers. While the tracking code does a good job of selecting the track that formed the trigger, there can be confusion in the tracking for overlapping events. The time window over which this could cause problems is 200-300 ns. For these measurements, the rates are low enough that we can reliably correct for these small (<1%) effects.

The uncertainty in the luminosity comes mainly from the measurement of the beam current and corrections for fluctuations in the target density. Because the rates are never too large, we can take all of the data at a fixed beam current. Thus, while the absolute uncertainty in the BCM calibration is about 0.5%, the fluctuation over time can be held to 0.2%. The density fluctuations due to heating are small for the present target and raster ($\sim 1\%$ at 100 μA) and should be nearly constant for fixed beam current.

At low Q^2 , the elastic rate over the full solid angle varies from 6 kHz at low beam energy to 14 kHz at high beam energy. However, the inelastic backgrounds are larger at forward angles so the raw event rate should vary by less than a factor of two. The *maximum* raw event rate will be roughly 25 kHz, leading to a small total correction for electronic deadtime ($\sim 0.1\%$) and multiple tracks ($\sim 0.7\%$), with an ε dependence that is less than half of this size. The uncertainties on these corrections will be less than 0.05%.

Significant systematic uncertainties can come from the uncertainty in the scattering kinematics, and so we will require beam energy measurements at each setting. The cross sections typically changes by 4–6% for a one percent change in beam energy, with little ε dependence. So an overall offset of 0.04% in the beam energy yields a scale uncertainty in the cross section of 0.2%, and an ε -dependent correction of 0.1%, very nearly linear in ε . The linearity measurement is much more sensitive to uncorrelated beam uncertainties. Assuming a point-to-point beam energy uncertainty of 0.04%, as obtained by E94-110 [32], the cross sections vary by about 0.2%.

The uncertainty in the angle of the scattered proton also breaks down into an overall offset (identical for both forward and backward angles) and an offset that can vary randomly as the spectrometer angle is changed. We expect to achieve an overall offset of 0.3 mr, somewhat larger than the 0.2 mr achieved in E94-110, due to the additional uncertainty associated with the software-defined solid angle. We may be able to do somewhat better since we can use the elastic scattering kinematics at each setting as a check on the angle offset. As seen in Fig. 8, a fixed offset yields a change in slope of 1% per mr, but maximum deviations from

linearity of only 0.2% per mr. So a 0.3 mr offset yields a linear ε dependence of 0.3%, which contributes to the uncertainty in G_E/G_M , but yields deviations from linearity of $<0.1\%$. For the linearity measurement, we are again more sensitive to angle offsets that vary randomly with changing scattering angles. E04-110 [32] achieved point-to-point uncertainties in the scattering angle of 0.2 mr. The sensitivity to the proton angle varies from 0.5–1.5% per mr, yielding uncertainties in the cross section of 0.1–0.3% (largest at large ε).

E. Kinematics

A precise measurement of any nonlinearities will require taking data at many ε values, including several low and high ε points. Figure 10 shows the kinematics (Q^2 vs. ε) for elastic scattering at the proposed energies. The green lines correspond to $E_{linac}=887$ (solid), 942 (dashed), and 1002 (dotted) MeV per pass, while the light blue lines correspond to 1067 (solid), 1133 (dashed), and 1200 (dotted) MeV per pass. While we have chosen to match the linac settings to those of E02-010, the experiment is compatible with other experiments that require several linac settings, although the specific Q^2 values at which we could make measurements would be slightly modified.

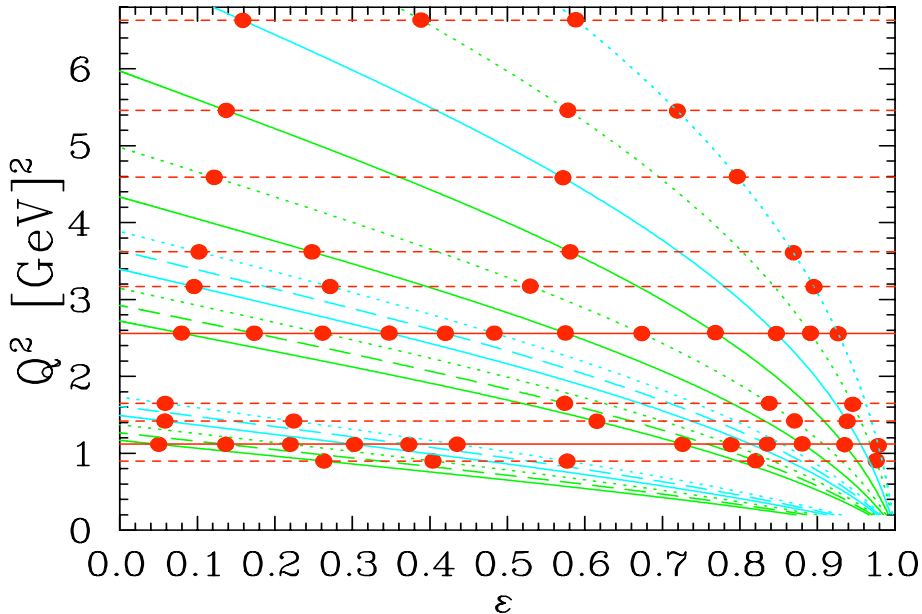


FIG. 10: The ε values that can be measured as a function of Q^2 for the available electron energies. The solid red lines indicate the Q^2 values where the nonlinearity measurements will be performed (12 ε values each), while the dashed lines indicate the additional Q^2 values where we will make precise measurements of G_E/G_M . The red circles indicate the points where measurements will be taken. The minimum ε value is determined by the minimum scattering angle of 10.5 degrees.

We propose to measure several points at twelve ε -values for $Q^2=1.12$ and 2.56 GeV². For

the low (high) Q^2 point, we will take one-pass (two-pass) data for each of the linac settings to provide six low ε points, and then take data at six high ε values, spaced roughly uniformly up to the maximum possible value. This will provide maximum sensitivity, especially if the nonlinearities occur only at extreme ε values. This will also allow us to precisely determine the slope in the linear region, and then see the effect of any nonlinearities in *multiple* data points. In addition to the linearity measurements, we will make precise extractions of G_E/G_M at $Q^2=0.90, 1.42, 1.65, 3.17, 3.62, 4.59, 5.46,$ and 6.63 GeV². These data will significantly improve the existing Rosenbluth extractions of $\mu_p G_E/G_M$, and allow us to use the discrepancy between Rosenbluth and polarization to make quantitative statements on the size of the two-photon amplitudes (Sec.V B).

F. Beam time request

Data taking for the points shown in Fig. 10 is summarized in Table III. We request a total of 13 PAC days, including the main data taking, calibration and checkout runs, and overhead for beam energy and changes.

$Q^2=0.90$ (0.1% statistics)	5×1 hr	5 hrs	
$Q^2=1.12$	12×1.5 hrs	18 hrs	
$Q^2=1.42$	5×1.5 hrs	8 hrs	
$Q^2=1.65$	4×2 hrs	8 hrs	
$Q^2=2.56$ (0.2% statistics)	12×2.5 hrs	30 hrs	
$Q^2=3.17$	4×3 hrs	12 hrs	
$Q^2=3.62$	4×4 hrs	16 hrs	
$Q^2=4.59$ (0.3% statistics)	3×4 hrs	12 hrs	
$Q^2=5.46$ (0.4% statistics)	3×5 hrs	15 hrs	
$Q^2=6.63$ (0.4% statistics)	3×8 hrs	24 hrs	148 hrs
Coincidence runs	3×6 hrs	18 hrs	
Target boiling studies		4 hrs	
BCM calibrations		8 hrs	
Checkout/calibration		12 hrs	
Beam energy measurements	18×1 hr	18 hrs	60 hrs
linac changes	6×8 hrs	48 hrs	
pass changes	12×4 hrs	48 hrs	96 hrs
Total			304 hrs (13 days)

TABLE III: Beam time request. Times listed for the main data taking include running on the dummy target and kinematic changes.

While the main data taking uses the hydrogen target, data taken on an aluminum

‘dummy’ target will be used to subtract the contributions from the target endcaps. We will also take runs at different beam currents to verify our measurement of the target heating effects, dead time, and other rate-dependent effects in the spectrometers. Data will be taken with a thin carbon target at all kinematics as a check on the target position and beam offsets. Finally, coincidence data will be taken at some settings as a check of the scattering kinematics, and as a measure of proton detection efficiency and absorption (although these corrections cancel in the ε dependence). We can also use the coincidence data to examine the elastic proton spectrum without the backgrounds, allowing us to check the agreement between the data and the simulated elastic (and background) spectra.

V. PROJECTED RESULTS FOR THE PROPOSED MEASUREMENTS

A. Projected Uncertainties (linearity and G_E/G_M)

Table II summarizes the systematic uncertainties for the measurements. Separate entries are given for the total uncertainty in the absolute cross sections, the uncertainties that enter into the extraction of G_E/G_M (neglecting ε -independent uncertainties), and the uncertainties that enter into the linearity tests (neglecting the portions of the systematic uncertainties that vary *linearly* with ε). Figure 11 shows the projected uncertainties for the proposed measurements of $\mu_p G_E/G_M$ compared to existing Rosenbluth and polarization transfer data. Note that the results are plotted as $(\mu_p G_E/G_M)^2$ as well as $\mu_p G_E/G_M$. This is the more accurate way of representing the Rosenbluth uncertainties, and it is these uncertainties that currently limit the extraction of the TPE amplitudes.

Figure 12 shows the kinematics for the linearity checks, along with the projected uncertainties, placed on different estimates of the two-photon corrections as described in section III. At $Q^2 = 2.64 \text{ GeV}^2$, the uncertainty (δP_2) on the quadratic term P_2 (Eq. 1) is 0.020, which yields a 4σ measurement using the estimate based on the calculation of Blunden, et al., [8], a 3.5σ measurement using the estimate of Afanasev, et al. [14], and a 6σ measurement based on the calculation from Chen, et al., [15]. For the $Q^2 = 1.12 \text{ GeV}^2$ measurement, $\delta P_2 = 0.018$, and P_2 is four or more standard deviations from zero for all three estimates. For the real data, the statistical scatter of the data points will change the extracted value of P_2 , but not the uncertainty on P_2 .

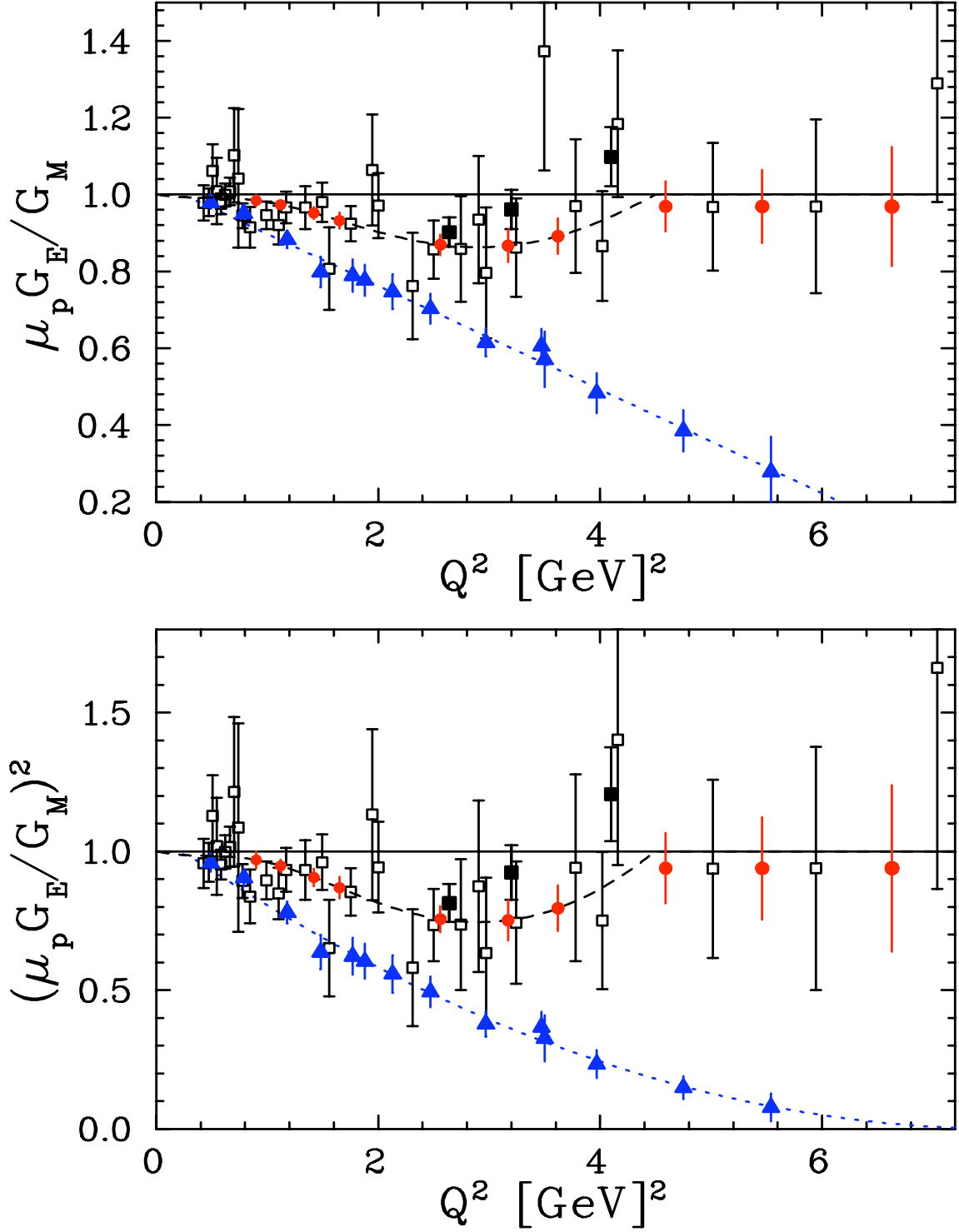


FIG. 11: Form factor ratio (top) and ratio squared (bottom) as deduced from polarization transfer (blue triangles), a global analysis of Rosenbluth separation experiments [10] (hollow squares), and from E01-001 (solid squares). The red circles show the projected uncertainties for this proposal. Note that the low Q^2 polarization transfer data shown are from the unpublished final analysis [35], and so show the anticipated final uncertainties.

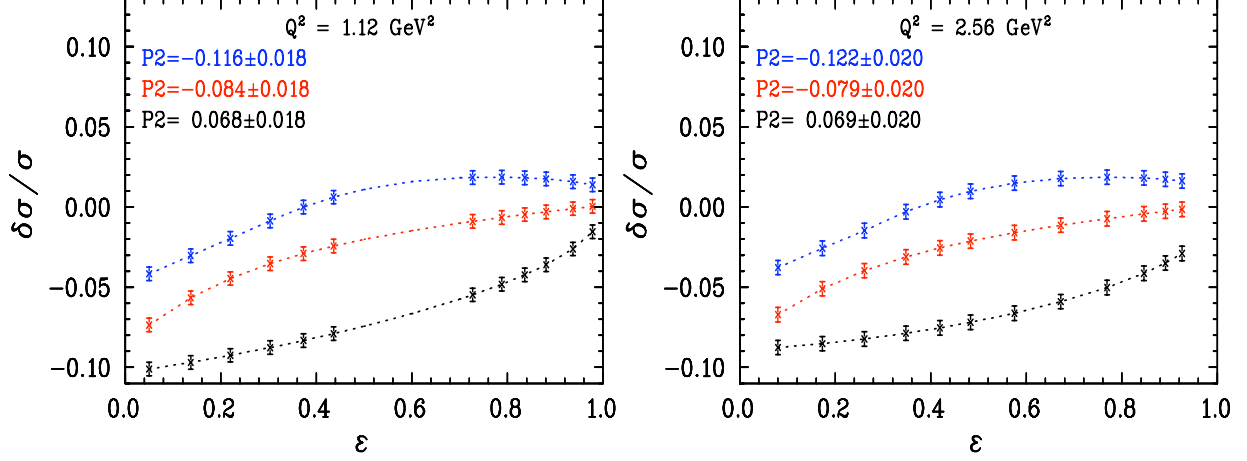


FIG. 12: The ε dependence of the two-photon contributions to the elastic e - p cross section from calculations by Blunden, et al., [8] (red), Afanasev, et al. [14] (black), and Chen, et al., [15] (blue), all scaled to explain the discrepancy as described in Fig. 6. The crosses show the kinematics and projected uncertainties for the proposed $Q^2 = 1.12 \text{ GeV}^2$ measurement (left) and the $Q^2 = 2.56 \text{ GeV}^2$ (right). For each curve, the extracted P_2 and its uncertainty are also shown.

B. Extraction of two-photon amplitudes

This section summarizes the extraction of the two-photon amplitudes presented in Ref. [9] (an extension of the work of Ref. [7]) and discusses the impact of the proposed measurements on this kind of analysis.

Using the formalism of Guichon and Vanderhaeghen [7], it is possible to express the cross section and polarization transfer results in terms of three generalized form factors, \tilde{G}_E , \tilde{G}_M , and \tilde{F}_3 , which include two-photon contributions, rather than the usual G_E and G_M that appear in the Born approximation. Note that these form factors depend on both ε and Q^2 . In this analysis [9], it is assumed that the TPE amplitudes are independent of ε . We will discuss the uncertainties related to this assumption at the end. For convenience, the generalized electric and magnetic form factors are broken up into the Born form factors and a two-photon contribution:

$$\tilde{G}_E(\varepsilon, Q^2) = G_E(Q^2) + \Delta G_E(\varepsilon, Q^2), \quad (2)$$

$$\tilde{G}_M(\varepsilon, Q^2) = G_M(Q^2) + \Delta G_M(\varepsilon, Q^2), \quad (3)$$

and we take

$$Y_{2\gamma} = \mathcal{R}e\left(\frac{\nu \tilde{F}_3}{M_p^2 |G_M|}\right), \quad (4)$$

where $\nu = M_p^2 \sqrt{(1+\varepsilon)/(1-\varepsilon)} \sqrt{\tau(1+\tau)}$ (equivalent to the definition given in Ref. [7]).

The ratio that is extracted from Rosenbluth and polarization transfer experiments (assuming one-photon exchange) can be written in terms of these generalized form factors, keeping terms up to order α with respect to the Born cross section, as

$$R_{Pol} = (\tilde{G}_E/\tilde{G}_M) + (1 - \frac{2\varepsilon}{1+\varepsilon}\tilde{G}_E/\tilde{G}_M)Y_{2\gamma}, \quad (5)$$

$$R_{Ros}^2 = (\tilde{G}_E/\tilde{G}_M)^2 + 2(\tau + \tilde{G}_E/\tilde{G}_M)Y_{2\gamma}, \quad (6)$$

and the change to the reduced cross section is

$$\frac{\Delta\sigma_r}{G_M^2} \approx 2\tau\frac{\Delta G_M}{G_M} + 2\varepsilon\rho^2\frac{\Delta G_E}{G_E} + 2\varepsilon(\tau + \rho)Y_{2\gamma}, \quad (7)$$

where $\rho = G_E/G_M$.

From Eqs. 5 and 6, we see that only the $Y_{2\gamma}$ term leads to a difference between the polarization transfer and Rosenbluth form factor ratios. This difference can therefore be used to determine $Y_{2\gamma}$ [7, 9]. To obtain the true form factors we must also determine ΔG_M and ΔG_E . Because the two-photon correction changes sign for positron–proton scattering, we can use the existing positron data to constrain ΔG_E and ΔG_M , allowing an extraction of the true form factors, G_E and G_M , corrected for two-photon (and multi-photon) exchange contributions. These are form factors that can be directly connected to the structure of the proton, and which can be compared to models of the nucleon.

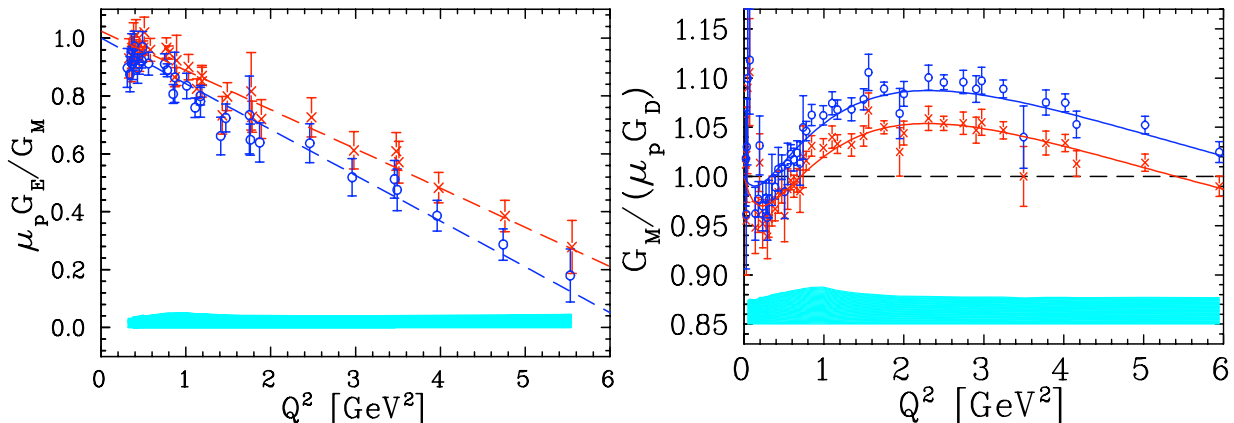


FIG. 13: Values of $\mu_p G_E/G_M$ (left) and G_M (right) as measured (red ‘x’) and after applying the TPE corrections as extracted from Ref. [9] (blue circles). The light blue band at the bottom of each figure shows the uncertainty on the TPE correction. For G_M , the largest uncertainties come from the extraction of the TPE amplitudes and the extrapolation to $\varepsilon = 0$ given the possibility of nonlinear behavior of the reduced cross section. For G_E/G_M , any ε dependence in the TPE amplitudes would modify the extracted amplitudes, and this model dependence has *not* been included in the error bands.

Such an analysis has been performed for the existing Rosenbluth and polarization transfer data [9]. The results and uncertainties of this analysis are shown in Fig. 13. However, at

present, this analysis is severely limited by the quality of the existing data in the following ways:

(1) The analysis must assume that the entire discrepancy is related to higher-order radiative corrections such as two-photon exchange.

(2) The ε dependence of the two-photon amplitudes is unknown. Ref. [9] assumes that the amplitudes are independent of ε .

(3) The uncertainties on the Rosenbluth extractions of $\mu_p G_E/G_M$ dominate the uncertainties (40–100%) in the extraction of the two-photon amplitudes.

While this proposal does not directly impact the first of these issues, existing positron data and recent attempts to calculate the two-photon exchange effects certainly suggest that the discrepancy is related to TPE contributions. This proposal does address the other two limitations of such an analysis. We will provide significantly better Rosenbluth measurements of $\mu_p G_E/G_M$, which will reduce the uncertainty in the two-photon amplitudes from 40–100% down to $\lesssim 20\%$ over a wide range in Q^2 . This will yield uncertainties related to these corrections that are comparable to or smaller than the experimental uncertainties in the form factors. The uncertainty in the two-photon amplitudes is currently dominated by the large uncertainties in the Rosenbluth measurements of G_E/G_M , and this yields the largest uncertainty in the TPE correction to polarization transfer measurements of G_E/G_M . The extraction of G_M is limited by uncertainty in the extrapolation to $\varepsilon = 0$ coming from possible nonlinearities. These measurements will set improved limits on any nonlinearity, and will also provide high-precision data at extremely low ε values, further reducing the uncertainty related to this extrapolation.

Figure 14 shows the values of $Y_{2\gamma}$ extracted from present measurements of G_E/G_M following the analysis of Ref. [9] along with the values and uncertainties that would be obtained from the proposed measurements, assuming that the ratio $\mu_p G_E/G_M$ is equal to unity. Table IV shows the uncertainties on G_M and G_E/G_M due to the experimental errors and the uncertainty in the TPE effects. The uncertainty shown for the *extraction* of the two-photon amplitudes assumes that the amplitudes are ε -independent. Any ε dependence would yield additional uncertainty, which would be reduced by the measurements proposed here.

Note that the assumptions used in Ref. [9] for the ε dependence of the TPE amplitudes is not unique. While assuming that ΔG_E , ΔG_M , and $Y_{2\gamma}$ are independent of ε satisfies the requirement that the effect on the cross section is linear, we only know that the correction is approximately linear, and relatively large deviations from linearity are allowed by the present data. In addition, there are other assumptions one can make that would also satisfy

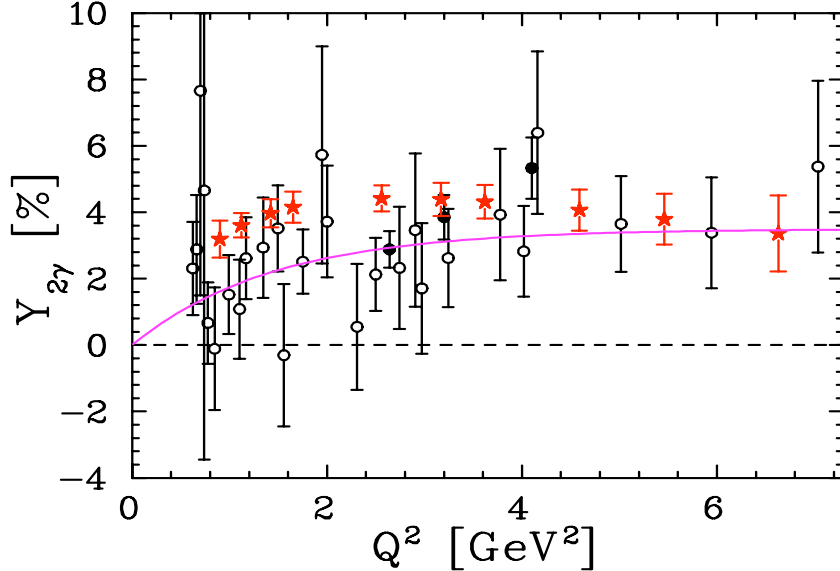


FIG. 14: Values of $Y_{2\gamma}$ extracted from various Rosenbluth measurements. Hollow circles are from conventional Rosenbluth separations, solid circles are from the E01-001, and the red stars indicate the projected uncertainties for this proposal. For the projected results, we assume $\mu_p G_E/G_M = 1$ for the new Rosenbluth results, and compare to the polarization transfer parameterization: $\mu_p G_E/G_M = 1 - 0.135(Q^2 - 0.24)$. We do not include the uncertainty in the polarization transfer measurements, which are negligible for large Q^2 , but comparable to the projected Rosenbluth uncertainties for $Q^2 < 2 \text{ GeV}^2$.

Form Factor	Source of uncertainty		
	Experimental	Extraction of 2γ amplitudes	Nonlinearities and e^+/e^- limits
G_M (current)	1-2%	*2-3%	2-3%
G_M (proposed)	1-1.5%	$\sim 1\%$	$\sim 0.5\%$
G_E/G_M (current)	4-10%	*6-13%	-
G_E/G_M (proposed)	4-10%	4-8.5%	-
* - Neglecting the uncertainty due to possible ε dependence on the <i>extraction</i> of the amplitudes			

TABLE IV: Experimental and two-photon exchange related uncertainties in the form factors given the existing data and with the inclusion of the proposed measurements.

this requirement. In the JLab E04-019 proposal [36], they assumed $\Delta G_E = \Delta G_M = 0$ and $Y_{2\gamma} = A + B/\varepsilon$. This also yields a linear correction to the cross section, but with very large values for $Y_{2\gamma}$ at small epsilon values ($Y_{2\gamma} \rightarrow \infty$ as $\varepsilon \rightarrow 0$). In addition, because there are multiple amplitudes, it is possible to have almost arbitrary ε dependence in a given amplitude, as its nonlinear effect on the cross section can be cancelled by other amplitudes which have little effect on polarization transfer observables. An extreme ε dependence to the

TPE amplitudes cannot be ruled out, and could yield very different effects on the polarization transfer extraction of G_E , as well as the Rosenbluth extraction of G_M . Thus, it is necessary to constrain the ε dependence of both polarization transfer and the reduced cross section.

VI. EXPERIMENTS WITH SIMILAR PHYSICS GOALS

Experiment E04-019 [36] was approved by PAC25 to measure the ε dependence of polarization transfer extractions of G_E/G_M . This is sensitive to the ε dependence of the two-photon amplitude $Y_{2\gamma}$. The discrepancy can be explained with small values of $Y_{2\gamma}$, well below the sensitivity of the experiment as proposed, but E04-019 will be able to determine if there is a large ε dependence in $Y_{2\gamma}$, or set upper limits if no effect is observed. Because the experiment will determine the ε dependence but not the *size* of $Y_{2\gamma}$, it will not by itself provide enough information to correct the polarization transfer results for two-photon effects. However, any information on the ε dependence of $Y_{2\gamma}$ can be used in the global analysis described above.

There are plans to make additional positron measurements to study TPE at Novosibirsk [23] and JLab [24]. These positron measurements cannot reach the larger Q^2 values where there is a clear discrepancy between Rosenbluth and polarization transfer, but they will allow us to verify that TPE is responsible for the discrepancy and to make precise measurements of TPE at low Q^2 values. We have assumed in this proposal that the discrepancy is due to TPE corrections. If it were shown that the discrepancy was caused by some problem with the polarization transfer data and that the Rosenbluth results were not significantly modified by two-photon effects, then the proposed measurements would only measure TPE through the linearity measurements, but would provide a dramatic improvement in the extraction of G_E over a large range in Q^2 (Fig. 11).

VII. CONCLUSIONS

We request a total of 13 days to perform high precision linearity checks at two Q^2 values, and high-precision Rosenbluth extractions of G_E/G_M at several Q^2 values from 0.9 to 6.6 GeV². Deviations from linearity would be a clear indication of deviation from the Rosenbluth formalism, and would provide valuable constraints on models of the two-photon exchange. Various calculations of the two-photon exchange corrections, small enough to be unobserved by previous measurements but large enough to explain the discrepancy between Rosenbluth and polarization transfer, yield very different nonlinearities which can be

observed as more than three to four standard deviation effects at both Q^2 values. Excluding the ε -dependence from Ref. [13], which appears to be ruled out, the different models shown in Fig. 6 differ by up to ten times the sensitivity of the best linearity measurement proposed here, and nearly twenty times the combined limit on nonlinearity from all of the measurements.

In addition, high precision Rosenbluth separations of G_E/G_M will be performed at several Q^2 values, allowing precise extractions of G_E/G_M from 0.9–6.6 GeV². Such high precision data can be compared to high precision polarization transfer data to determine the magnitude of the two-photon corrections as a function of Q^2 . At large Q^2 values, the ε dependence comes almost entirely from TPE, and so Rosenbluth measurements in this region are almost as clean a measurement of TPE effects as comparisons of positron and electron scattering. With these data on the ε and Q^2 dependence of the two-photon exchange amplitudes, we can extract the TPE amplitudes and use these to correct the measured proton form factors. At present, lack of knowledge of the TPE effects yields a 3–5% uncertainty on G_M , which had been assumed to be known at the 1–2% level. The TPE corrections to polarization transfer dominate the uncertainty in our knowledge of G_E , especially at large Q^2 values. With the proposed measurements, a global analysis of Rosenbluth, polarization transfer, and positron measurements will allow us to extract the two-photon amplitudes at the $\sim 20\%$ level rather than the 50–100% level. This level of precision is enough to correct the measured form factors with an uncertainty on TPE effects that is at or below the experimental uncertainties of the data.

The impact of these data extends beyond our knowledge of the proton form factors. It is important to understand both the form factors and TPE effects for precision experiments which rely on knowledge of either the elastic cross section or the proton form factors. It is also important to have adequate experimental data with which to constrain calculations of two-photon exchange. Elastic e - p scattering is the only case where it is currently possible to study TPE, and these same corrections must also be important for radiative corrections in e - n and e - A elastic scattering, measurements of transition form factors, and in the parity-violating interference terms between photon and Z exchange. For all of these cases, we can only make theoretical estimates of the effects of these higher-order diagrams, and so it is vital to study such estimates in the unique case of e - p scattering, where we have good experimental access to the effect of TPE.

[1] R. C. Walker et al., Phys. Rev. D **49**, 5671 (1994).

- [2] P. E. Bosted, Phys. Rev. C **51**, 409 (1994).
- [3] M. K. Jones et al., Phys. Rev. Lett. **84**, 1398 (2000).
- [4] O. Gayou et al., Phys. Rev. Lett. **88**, 092301 (2002).
- [5] J. Arrington, Phys. Rev. C **68**, 034325 (2003).
- [6] I. A. Qattan et al. (2004), nucl-ex/0410010.
- [7] P. A. M. Guichon and M. Vanderhaeghen, Phys. Rev. Lett. **91**, 142303 (2003).
- [8] P. G. Blunden, W. Melnitchouk, and J. A. Tjon, Phys. Rev. Lett. **91**, 142304 (2003).
- [9] J. Arrington (2004), hep-ph/0408261, accepted for publication in Phys. Rev. C.
- [10] J. Arrington, Phys. Rev. C **69**, 022201(R) (2004).
- [11] D. Higinbotham, Tech. Rep., JLab Report JLAB-PHY-03-116 (2003).
- [12] J. Arrington and I. Sick, Phys. Rev. C **70**, 028203 (2004).
- [13] M. P. Rekalo and E. Tomasi-Gustafsson, Eur. Phys. J. **A22**, 331 (2004).
- [14] A. Afanasev, S. Brodsky, and C. Carlson, presented at the Oct. 2003 DNP Meeting.
- [15] Y. C. Chen, A. Afanasev, S. J. Brodsky, C. E. Carlson, and M. Vanderhaeghen, Phys. Rev. Lett. **93**, 122301 (2004).
- [16] K. G. Fissum et al. (Jefferson Lab Hall A), Phys. Rev. **C70**, 034606 (2004).
- [17] D. Dutta et al., Phys. Rev. C **68**, 064603 (2003).
- [18] K. A. Aniol et al. (HAPPEX), Phys. Rev. **C69**, 065501 (2004).
- [19] H. Budd, A. Bodek, and J. Arrington (2003), hep-ex/0308005.
- [20] J. Mar et al., Phys. Rev. Lett. **21**, 482 (1968).
- [21] L. Camilleri et al., Phys. Rev. Lett. **23**, 149 (1969).
- [22] J. Arrington, Phys. Rev. C **69**, 032201(R) (2004).
- [23] J. Arrington, D. M. Nikolenko, et al., Proposal for positron measurement at VEPP-3, nucl-ex/0408020.
- [24] W. Brooks, A. Afanasev, J. Arrington, K. Joo, B. Raue, L. Weinstein, et al., Jefferson lab experiment E04-116.
- [25] L. Andivahis et al., Phys. Rev. D **50**, 5491 (1994).
- [26] R. R. Lewis, Phys. Rev. **102**, 537 (1956).
- [27] S. D. Drell and M. Ruderman, Phys. Rev. **106**, 561 (1957).
- [28] S. D. Drell and S. Fubini, Phys. Rev. **113**, 741 (1959).
- [29] N. R. Werthammer and M. A. Ruderman, Phys. Rev. **123**, 1005 (1961).
- [30] G. K. Greenhut, Phys. Rev. **184**, 1860 (1969).
- [31] W. Melnitchouk, private communication.
- [32] M. E. Christy et al., Phys. Rev. C **70**, 015206 (2004).
- [33] J. Litt et al., Phys. Lett. B **31**, 40 (1970).
- [34] C. Berger, V. Burkert, G. Knop, B. Langenbeck, and K. Rith, Phys. Lett. B **35**, 87 (1971).
- [35] V. Punjabi et al., Tech. Rep., JLab Report JLAB-PHY-03-13 (2003).
- [36] R. Gilman, L. Pentchev, C. Perdrisat, R. Suleiman, et al., Jefferson lab experiment E04-019.